

Scientific impact of the standard phase reconstruction method and its clinical applications

Yu-Chen Huang¹, Aymen Alian², Yu-Lun Lo¹, Kirk Shelley², Hau-Tieng Wu^{3,4}

1. *Department of Thoracic Medicine, Chang Gung Memorial Hospital, Chang Gung University, College of Medicine, Linkou, Taiwan*
2. *Department of Anesthesiology, Yale University, New Haven, CT, USA*
3. *Department of Mathematics and Department of Statistical Science, Duke University, Durham, North Carolina, USA*
4. *Mathematics Division, National Center for Theoretical Sciences, Taipei, Taiwan*

Corresponding Authors:

Hau-Tieng Wu, MD PhD, Associate Professor of Department of Mathematics and Department of Statistical Science, Duke University, 140 Science Drive, Durham, NC 27705, USA. Email: hauwu@math.duke.edu

Abstract

Phase is the most fundamental physical quantity when we study an oscillatory time series, and there are a lot of tools aiming to estimate phase. Most existing tools are developed based on the well-developed analytic function model. Unfortunately, this approach might not be suitable for several modern signals, particularly biomedical signals, due to the intrinsic complicated structure, and the lack of standard methods on how to estimate phases. Specifically, different recording equipment for the same physiological system might lead to different phases based on existing

tools, and the same recording equipment for different subjects might vary from subject to subject, even if the cycling periods are the same. The lack of consensus, or standard, might lead to the challenge of reproducibility, communication, and scientific interpretation. In face of this challenge, we propose the use of the recently developed adaptive non-harmonic model and synchrosqueezing transformation to standardize the phase information extraction. To illustrate the scientific impact of the proposed standardization and tools, we show analysis results in two different physiological signals with clinical applications.

1. Introduction

Phase is the most fundamental physical quantity when we study an oscillatory (or periodic) signal. It has been studied over centuries and is a standard material covered in signal processing, communication, physics, and almost all scientific related fields. In the layman's language, the phase of an oscillatory signal is the *relative value* of the signal within the span of a *single* oscillatory period (Figure 1a). It is closely related to the notion of frequency and period. In biomedicine, the phase contains crucial physiological information; for example, the pulse transit time is the phase relationship between the electrocardiogram (ECG) and the photoplethysmogram (PPG), and it reflects the blood pressure [1, 2]; the coupling between the heart and lung, usually known as the cardiopulmonary coupling (CPC), is quantified by evaluating the relationship between the phases of the heart rate and respiratory signal [3]; the coupling between different frequency bands of the electroencephalogram (EEG) has been well explored in the neuroscience society [4, 5]

Historically, there has been rich literature discussing theoretical foundation of phase function, for example [6-10], which is far from an exhaustive list. The widely accepted model for the phase function is the *analytic function* model [6, 10, 11] proposed by Gabor back in 1946 [10], based on which most existing theory and phase extraction algorithms are developed. The Hilbert

transform [12] with or without a bandpass filter design or its variations [13], time frequency (TF) analysis tools like continuous wavelet transform (CWT) [14] or others [15, 16], Blaschke decomposition [18] or adaptive Fourier transform [17], or even empirical mode decomposition [19], are commonly applied algorithms. This analytic function model and associated algorithms (hereafter called *traditional approach*) have been successfully applied to various scientific fields, like the communication system.

However, in biomedicine, depending on the signals, this traditional approach might be limited. For example, it has been a standard and widely applied [20], and it is claimed in Le Van Quyen M., et al. [21] that there are minor differences between the Hilbert transform and CWT on the intracranial or scalp EEGs. However, for other oscillatory physiological signals, like the respiratory signal, PPG and peripheral venous pressure (PVP) [42], its application might be problematic due to the non-sinusoidal pattern and time-varying frequency and amplitude. Moreover, even for the same sensor, the oscillatory patterns may vary from one subject to another, or even from time to time on the same subject, and this varying oscillatory pattern further impacts the estimated phase if we apply the traditional approach.

A critical question to ask for the biomedical research is if the traditional approach is suitable, and in what sense. To properly answer the question, we need to have a consensus on the phase function. To the best of our knowledge, while it has been well answered in, for example, the radio engineering in communication or information processing, this topic is not systematically discussed in biomedicine, except some reports [21]. The lack of consensus, or standard, might lead to the challenge of reproducibility, communication, and scientific interpretation.

Inspired by this scientific need, we provide a standardization of the phase function estimation in this article. We start from modeling an oscillatory biomedical time series. This model generalizes the traditional analytic function model and offers a platform to standardize the definition and interpretation of what a phase function should be. We then advocate estimating the

standardized phase by a novel nonlinear-type TF analysis tool, the synchrosqueezing transform (SST) [22, 23]. The proposed standardization resolves the above-mentioned limitations and have various immediate applications, including information sharing, discussion of the scientific findings among different equipment, etc. We demonstrate how to apply the proposed standardization by analyzing two clinical databases.

2. What is phase? A standardization of the terminology and model

To determine the phase of an oscillatory biomedical time series, we face the following fundamental question – what is phase? We describe existing models and introduce the proposed standardized one. A summary of the relationship among these models can be found in Figure 1b.

2.1. Harmonic function

In the textbook setup [12], for a given oscillatory time series, common features associated with the oscillatory behavior are the frequency, which represents how fast the signal oscillates, the amplitude, which represents how strongly the signal oscillates at that frequency, and phase shift. Mathematically, this oscillatory signal is expressed by the *harmonic function*:

$$F(t) = ae^{i(2\pi\xi t + \varphi)}, \quad (1)$$

where $a > 0$ is the amplitude, $\xi > 0$ is its frequency, and φ is the *phase shift*, which is a number between 0 and 2π . We call the function $\xi t + \varphi$ the *phase function*, which physically describes the status of an oscillation at time t . See Figure 2a for an example, where we use the Euler's formula to represent $F(t)$ in its real and imaginary parts. Given $F(t)$, it is transparent to evaluate the phase function directly by *unwrapping* the function $\frac{F(t)}{|F(t)|} = \frac{F(t)}{a} = e^{i(2\pi\xi t + \varphi)}$ by finding the angle of

the complex number $e^{i(2\pi\xi t + \varphi)}$. Usually, the signal we record is real-valued; that is, the signal is usually of the format

$$f(t) = \text{acos}(2\pi\xi t + \varphi) \quad (2)$$

with the same meaning and condition for a , ξ , and φ . A common practice is applying the Hilbert transform to convert $f(t)$ to $F(t)$, and then get the phase function.

2.2. Generalization of harmonic function

In practice, however, most physiological signals are not harmonic since they oscillate with time-varying frequency and amplitude. For example, a subject might breathe at different rate at different moments [24]. We propose to quantify this behavior by the following mathematical model:

$$F_0(t) = A(t)e^{i2\pi\varphi(t)}, \quad (3)$$

where $A(t)$ is a smooth positive function and $\varphi(t)$ is a smooth monotonically increasing function. We call $\varphi'(t)$, the derivative of $\varphi(t)$, the *instantaneous frequency* (IF) and $A(t)$ the *amplitude modulation* (AM) of the function $F_0(t)$ [23]. The phase function we are concerned with in this paper is defined as $\varphi(t)$. See Figure 2a for an example. Clearly, (1) is a special case of (3) when the AM is a positive constant function, the IF is a positive constant function, and the phase is a linear function. Physically, at time t , the signal $F_0(t)$ repeats itself in about $1/\varphi'(t)$ seconds with the oscillatory magnitude $A(t)$. This function has been shown to well approximate several physiological signals [25, 26]. For this model, since $|F_0(t)| = A(t)$, the phase can be easily uniquely evaluated by unwrapping $\frac{F_0(t)}{|F_0(t)|} = e^{i2\pi\varphi(t)}$.

In practice, the signal is real and satisfies

$$f_0(t) = A(t)\cos(2\pi\varphi(t)), \quad (4)$$

and the meanings of $\varphi'(t)$, $\varphi(t)$, and $A(t)$ are the same that those in (3). Unlike the relationship between (1) and (2), we face the first challenge in evaluating the phase function, which sometimes is called the *Vakmans' problem* [27-29]. The usual practice is applying the Hilbert transform to recover $F_0(t)$ from $f_0(t)$; however, it is not usually mathematically correct. First, $F_0(t)$ is *not* an analytic function, nor a unitary function [6]. Moreover, the Hilbert transform cannot recover $F_0(t)$ unless some specific conditions are satisfied [9, 30], but these conditions are limited [6] and might not be practically possible.

We emphasize that the model could be *physically accurate* and widely applied while not mathematically correct [6]; for example, the frequency modulation with high carrier frequency model in the radar communication. However, for the biomedical time series, this model might also be physiologically inaccurate, and hence in general the phase defined under the model (3) cannot be applied or even correctly interpreted. See Figures 4a and 6a for examples.

Despite the above limitations, it has been found that with some reasonable conditions, we can move forward with the model (4). A reasonable condition is the *slowly varying AM and IF* [22, 23]; that is, the AM and IF change slowly compared with the IF. When this condition is satisfied, (4) is called the *intrinsic mode-type function* (IMT). This model reflects physiological homeostasis – the variability from cycle to cycle does not change dramatically during a short time without external stimulations, while the system might migrate from one status to another over a long period. Under such a condition, it is shown in [22] that the phase can be uniquely defined up to a negligible error, and it does make sense to define the phase to be the same as that in the model (3).

2.3. More realistic model – multiple components and wave-shape function

We need to handle more challenges since there are detailed features that cannot be captured by the IMT function. One particular feature is the *non-sinusoidal* oscillatory pattern. For example, ECG or PPG usually do not oscillate like a sine wave. Moreover, usually a biomedical

signal is composed of several components with different physiological interpretations. For example, the PPG signal is composed of one hemodynamic component and one respiratory component known as the respiratory induced intensity variation (RIIV) [31]; the respiratory signal is composed of one respiratory component, and one hemodynamic component known as the cardiogenic artifact [32]. These observations lead to the following model: [33, 34]

$$f(t) = \sum_{l=1}^L f_l(t), \quad (5)$$

where

$$f_l(t) = A_l(t)s_l(\varphi_l(t)), \quad (6)$$

for each $l = 1, \dots, L$, $A_l(t)$ and $\varphi_l(t)$ have the same meanings as those in (3), and s_l is a real 1-periodic function with the unitary energy. We call $f_l(t)$ the l -th oscillatory component of the signal $f(t)$, and $s_l(t)$ the *wave-shape function* of the l -th oscillatory component. The model (5) is called the *adaptive nonharmonic model* (ANHM) [33, 34]. See Figure 2a for a simulated example with a non-sinusoidal oscillatory signal when $L = 1$, and Figures 2b and 2c for several physiological signals. Clearly, (5) is a generalization of (4). Indeed, when $L = 1$ and $s_1(t) = \cos(2\pi t)$, (5) is reduced to (4). This ANHM will be our base to standardize the definition of phase for a biomedical signal.

We start from the case when $L = 1$ in (5). Intuitively, $s(\varphi(t))$ in $f(t) = f_1(t) = A(t)s(\varphi(t))$ is nothing but “stretching” the periodic signal $s(t)$ by the monotonic signal $\varphi(t)$, and then “scaling” by the positive function $A(t)$. We thus define *the* phase function of $f(t)$ to be $\varphi(t)$. We need to mention a critical possible confusion point here. When the Hilbert transform is applied to $f_1(t)$, $f(t)$ can be written as the real part of $\tilde{a}(t)e^{i2\pi\tilde{\varphi}(t)}$, where if we enforced $\tilde{a}(t) > 0$, $\tilde{\varphi}(t)$ might *not* be a monotonic increasing function. In the traditional approach, the widely accepted definition of phase function of $f(t)$ as $\tilde{\varphi}(t)$. See a simulation in Figure 3 as an example of such model and approach. Note that the recovered phase function might be non-monotonic, and this approach is sensitive to the input signal, even if two signals shown in Figure 3 are “visually similar”. This fact

comes from the “winding” effect from the complex analysis perspective. This example demonstrates some challenges we might encounter when we use the analytic function model.

To look deeper into this phenomenon, recall a different interpretation of the signal $f(t) = f_1(t) = A(t)s(\varphi(t))$. When $s(t)$ is smooth enough, (5) could be expanded as by the Fourier series as

$$f(t) = A(t) \sum_{k=1}^{\infty} a_k \cos(2\pi k \varphi(t) + b_k), \quad (7)$$

where we assume $a_k > 0$, and set $a_k \geq 0$ for $k > 1$, b_k is between 0 and 2π , and $\sum_{k=1}^{\infty} a_k^2 = 1$ is the energy. If we rewrite (5) in the format of (7), the interpretation of $f(t)$ is different – it is an oscillatory signal with multiple *sinusoidal* oscillatory components. We follow the tradition in signal processing and call $a_k \cos(2\pi \varphi(t) + b_k)$ the *fundamental component* and $a_k \cos(2\pi k \varphi(t) + b_k)$, $k > 1$, the $(k - 1)$ -th *multiple (harmonics)* of the fundamental component. Clearly, the phase function $\varphi(t)$ we consider in this work is the phase function of the fundamental component, while the phase in the traditional approach, $\tilde{\varphi}(t)$, contains information not only from the fundamental component, but also from *all* harmonics. As a result, sometimes researchers apply a bandpass filter before applying the Hilbert transform. However, due to the time-varying frequency and amplitude, this approach might mix up spectral information of different components. In short, while the model (5) could model various physiological time series, traditional approach might not work as expected.

Now, we argue why it is better to define the phase to be $\varphi(t)$ instead of $\tilde{\varphi}(t)$ for $f(t) = f_1(t) = A(t)s(\varphi(t))$ by taking physiological knowledge into account. Take ECG signal as an example, where the IF, AM and the wave-shape function have their own physiological meanings. The wave-shape function of the ECG signal reflects the electrical pathway inside the heart, where the sensor is put, the heart anatomy, etc. Several clinical diseases are diagnosed by reading the wave-shape function but not reading its decomposition in (7). Moreover, while time moves forward, the physiological status should “move forward”; that is, the phase function should be monotonically increasing. This physiological fact, combined with the fact shown in Figure 4a,

suggests that it is better to separate the wave-shape function from the phase function as in (5), which is precisely our definition of the phase function. In summary, our phase function $\varphi(t)$ describes at which status the oscillation is at each time, where the status is described by the wave-shape function. It is thus a better choice than the phase function $\tilde{\varphi}(t)$, which is a mix-up of this status information and the wave-shape function. Our definition has more benefits from the perspective of IF and AM. In the ECG example, it is well known that while the rate of the pacemaker is constant, the heart rate generally is not constant. The discrepancy comes from neural and neuro-chemical influences on the pathway from the pacemaker to the ventricle. This non-constant heartbeat rate could be modeled as the IF of the ECG. Moreover, the AM of the ECG reflects the breathing activity via the thoracic impedance. If we take model (7) into account, the interpretation of IF and AM might not be physiological.

Finally, we discuss the case when $L > 1$. In the traditional approach, we may define the phase function $\tilde{\varphi}(t)$ via the Hilbert transform. But we may have interpretation problem even if $s_l(t) = \cos(2\pi t)$ for $l = 1, \dots, L$, since the phase information of different oscillatory components might be mixed-up. This leads to the same problem shown in Figure 3 discussed above, since the signal in (5) with $L = 1$ is a special case when written in (7). To resolve this issue, we propose to define the phase of (5) to be a collection of phase functions associated with oscillatory components; that is, given $f(t)$ in (5), the *phase function* is a set of phase functions $\varphi_l(t), l = 1, \dots, L$. Take the PPG as an example. Since the PPG is composed of two oscillatory components with different physiological contents, it makes perfect sense to describe the phase of each component separately. However, if we view these two oscillatory components together and define its phase in the traditional approach, it might be challenging to interpret what this phase function tells us.

In summary, we propose to use model (5) to describe various oscillatory physiological signals, and the associated phase function can be standardized and defined unambiguously with physiological meanings. We mention that since the first proposal was published in [33], there

have been several generalizations to capture different aspects of this kind of signals [34]. To avoid mathematical complications, we focus on (5) in this paper.

3. Methodology

We provide an algorithm to estimate the standardized phase function of the signal (5). The Matlab implementation is available in <http://hautiangwu.wordpress.com/>.

3.1. Synchrosqueezing transform

We summarize the SST algorithm, a novel nonlinear-type TF analysis tool [23], which sets the foundation for the phase estimation algorithm, and refer readers to an introductory article for more details [42]. Fix the Gaussian function $h(t) = e^{-t^2}$. In general, the window function $h(t)$ can be chosen to be anything that is smooth, centered at 0 and decays fast enough. The short time Fourier transform (STFT) [15,16] is carried out by the following formula

$$V^{(h)}(x, \xi) = \int f(t)h(t - x)e^{-i2\pi t\xi} dt, \quad (8)$$

where ξ is a scalar that means the frequency. When x is fixed, the function $V^{(h)}(x, \cdot)$ is the Fourier transform of $f(t)h(t - x)$, which is the truncated $f(t)$ by h centered at x . Mathematically, we call the set of pairs (x, ξ) the *TF domain*, and $V^{(h)}$ is the *TF representation* (TFR) of $f(t)$ via STFT.

Note that STFT provides a complex-valued function defined on the TF domain, and the angle of each complex value (also confusingly called phase) contains extra information about the signal.

Next, evaluate the *reassignment rule*

$$\Omega^{(h)}(x, \xi) = \frac{1}{i2\pi} \frac{\partial_x V^{(h)}(x, \xi)}{V^{(h)}(x, \xi)}, \quad (9)$$

when $V^{(h)}(x, \xi)$ is nonzero and $-\infty$ otherwise. Finally, reallocate STFT coefficients according to the reassignment rule:

$$S^{(h)}(x, \eta) = \int_0^\infty V^{(h)}(x, \xi) \delta_{|\eta - \Omega^{(h)}(x, \xi)|}(\xi) d\xi, \quad (10)$$

where $\eta > 0$ is the frequency and δ is the Dirac delta measure. $S^{(h)}$ is the TFR of $f(t)$ provided by SST. The main benefit of SST is enhancing the contrasts of TFR and alleviate the possible spectral mix-up between different components. The key ingredient of SST is the fact that the reassignment rule tells us how fast the signal oscillates at each time. Indeed, if $V^{(h)}(x, \xi) = |V^{(h)}(x, \xi)|e^{i\Phi^{(h)}(x, \xi)}$ is nonzero, we have $\log(V^{(h)}(x, \xi)) = \log(|V^{(h)}(x, \xi)|) + i\Phi^{(h)}(x, \xi)$. Since $\frac{\partial_x V^{(h)}(x, \xi)}{V^{(h)}(x, \xi)} = \partial_x \log(V^{(h)}(x, \xi))$, $\Phi^{(h)}(x, \xi)$ encodes “how much” the signal has oscillated at frequency ξ up to time x , and its derivative gives us how fast the signal oscillates at time x . SST has been widely studied, and there have been several generalizations of SST. We refer readers to [35] for a recent review of SST. For readers with interest in theoretical results and statistical inference, we refer them to [22, 23, 36].

3.2. Obtain the standardized phase

With the TFR of $f(t) = f_1(t) = A(t)s(\varphi(t))$ by SST, the phase can be estimated via the following two steps. First, suppose the TFR $S^{(h)}$ is discretized as a $N \times m$ matrix, where N means the number of signal sampling points, and m means the number of frequency bins. The fundamental frequency is extracted via [22]

$$c^* = \max_{c \in Z_m^N} \sum_{n=1}^N \log \left[\frac{|S^{(h)}(c(n), n)|}{\sum_{i=1}^m \sum_{j=1}^N |S^{(h)}(j, i)|} \right] - \lambda \sum_{n=2}^N |c(n) - c(n-1)|^2, \quad (11)$$

where $\lambda > 0$ is a parameter chosen by the user, $Z_m = \{1, 2, \dots, m\}$, and c^* is a N dim vector representing a curve on the TFR. In this work, we choose $\lambda=0.5$. The first term in this optimization fits the TFR with a curve that captures the most intense pixels in the TFR, while the second term imposes the smoothness constraint on the extracted curve. According to the established theory [22, 23], suppose the tick of the j th bin in the frequency axis is $j\Delta\xi$, the IF of the fundamental component at time $i\Delta t$ is $c^*(i)\Delta\xi$.

Next, we reconstruct the fundamental component:

$$\tilde{f}(i\Delta t) = \int_{c^*(i)\Delta\xi-\delta}^{c^*(i)\Delta\xi+\delta} S^{(h)}(i\Delta t, \zeta) d\zeta, \quad (12)$$

where $\delta > 0$ is chosen by the user. That is, at time $i\Delta t$, we sum up the frequency band centered at the IF $c^*(i)\Delta\xi$, with the bandwidth δ . In this work, we choose $\delta=0.1$. According to the established theory [22, 23], \tilde{f} well approximates the *complex* form of the fundamental component of the oscillation ingredient we have interest; that is, $\tilde{f}(t) = A(t)a_1 e^{i(2\pi\phi(t)+b_1)}$ up to a negligible error. Therefore, according to the model (6), since $A(t)a_1$ is not zero, the phase can be estimated by unwrapping $\tilde{f}(t)/|\tilde{f}(t)|$. We mention that from the filter theory perspective, this approach can be understood as a *time-varying band-pass filter*, where the band is determined in a local way, compared with the fixed band approach like that in the band-pass filter or CWT approaches. By repeating this procedure, we obtain the phase function of all oscillatory components when $L > 1$ in (5). In Figure 3, we illustrate the estimated phase of a simulated chirp signal with non-sinusoidal oscillation. Clearly, the trouble we encountered in the traditional approach is eliminated. As we will discuss below, even if the IFs of different components have separate ranges, it is not always a good idea to apply the bandpass filter, in particular when the signal oscillates with IF and AM.

Below, we demonstrate how to apply the proposed standardization and tools in two databases.

4. First testbed -- COPD

4.1. Material

The first database comes from a prospective study that recruits patients with a clinical diagnosis chronic pulmonary obstructive disease (COPD) according to the Global Initiative for Obstructive Lung Disease Criteria at Chang Gung Memorial Hospital (CGMH), Linkou, Taiwan, from January 2019 to December 2019. The ethics committee of CGMH approved the study. All participants signed informed consent before enrollment. Patients with heart failure (Ejection fraction <40%), lung cancer, atrial fibrillation, using anti-arrhythmic agents and using oxygen were

excluded. Total of 52 patients were included, with impaired pulmonary function test with FVC (Forced vital capacity) 81% (42%-130%) and FEV₁(Forced expiratory volume in 1st second) 60% (21-105%). Experiments were carried out in a quiet room with the temperature maintained at 22-24 °C. Patients were instructed to avoid bronchodilators such as beta-2 agonists, xanthene derivatives, alcohol and coffee before the experimental test. The skin was abraded with gel then cleaned with alcohol to reduce skin electrode impedance before ECG electrodes attachment. Before the examination, blood pressure, heart rate, and oxygen saturation were recorded. They wore the pulse oximeter on the finger and ECG electrodes on the chest wall. We recorded the flow signal for 5 minutes continuously. To avoid any signal quality issue, before the recording, the patient practiced breathing via the flow tube for 45 seconds. Three Actiwave devices were used for recording flow signal and ECG signal. Recording signals were transferred via European Data Format to LabChart 8 analysis software (ADInstruments, USA), and then exported to text files for analysis.

We will show how the estimated phase function influences the widely used algorithm called synchrogram proposed in [37] to quantify the CPC [38, 39]. The synchrogram is composed of two steps. First, calculate the phase functions of the instantaneous heart rate (IHR) and the respiratory signal. Then, quantify the phase locking by the stroboscope idea to depict the CPC. The R peaks are determined by the standard R peak detection algorithm, the impact of ventricular premature contraction is modified by the standard RRI correction algorithm [40], and the IHR is determined by the standard interpolation of R peak to R peak interval (RRI) time series.

4.2. Results

For each subject, we simultaneously recorded three respiratory signals, including flow, impedance, and end-tidal CO₂. See Figure 2b. It is clear that those signals have different morphologies encoding different physiological information, but their periods, or the length of respiratory cycles, are similar. As discussed above, the morphology is mainly captured by the multiples of the fundamental component. If this polymorphic behavior of respiratory signals is not

properly handled, the phase information might be contaminated. In Figure 4a, we show that with the bandpass filter (0.1-0.4 Hz) and the Hilbert transform, the phases of all signals “look close”. But once we take the derivative, the IF’s of all channels are different. Moreover, the IF’s are not physiologically sensible. In Figure 4b, we show the TFR of those signals. We can see a clear and dominant curve around 0.5 Hz in each TFR, which means that the IF’s of all signals’ fundamental components are consistent. The estimated phases and their derivatives are also consistent among all channels. Compared with Figure 4a, the results by SST are more sensible and consistent.

To further evaluate the benefit of the standardization, we claim that with the bandpass filter and the Hilbert transform, the CPC index determined by the synchrogram might vary from one respiratory signal to another. Obviously, this will limit scientific communication and reproducibility. We claim that this issue could be resolved by the proposed standardization and algorithm. The IHR, various respiratory signals, the associated TFRs determined by SST, and the associated synchrograms are shown in Figure 5a. It is clear that all TFRs share a common dominant curve. Also, note that while the three synchrograms might look different, actually they are similar up to a global phase shift that comes from the global phase shift inherited in the wave-shape functions. The Bland-Altman plots of the CPC indices of 52 subjects determined from different phase estimation methods and different respiratory signals are shown in Figure 5b. It is clear that if the phase is estimated by SST, the coupling index is less impacted by the sensor types compared with the Hilbert transform approach.

5. Second testbed -- LBNP

5.1. Material

The second database comes from a prospective study that recruits normal subjects for the lower body negative pressure (LBNP) experiment that simulates blood loss. After approval of the protocol by the Yale University Human Committee, 36 healthy subjects of both sexes with age

18-40 years were recruited and provided written consent. Exclusion criteria were current pregnancy or any history of pulmonary, cardiac, or vascular disease including hypertension effectively treated with antihypertensive medication. Subjects were instructed to refrain from alcoholic and caffeinated beverages, strenuous exercise, and tobacco consumption for at least 12 hours prior to the study. A negative pregnancy test was confirmed for all female subjects immediately before participation. Intravenous access was established as a precautionary measure, but fluids were not infused during the study. Each subject was monitored with various channels, but we only focus on the PPG and peripheral venous pressure (PVP) signal (Nonin Medical, Inc., Plymouth, MN). All data were digitized and continuously recorded to a laptop computer. Each procedure was performed in a climate-controlled laboratory at 72°F and 20% humidity. Details of the LBNP are well described [41]. Briefly, after the leg raising test and following a subsequent 5-minute equilibration period, the chamber was sealed to start the LBNP sequence. This entailed 3 minute phases during which the pressure was progressively decreased by 15 mmHg until either 3 minutes at -75 mmHg were completed or at any phase symptoms consistent with significant hypovolemia occurred including light headedness, nausea, diaphoresis, blurred vision, tingling in extremities, or a measured systolic blood pressure less than 80 mmHg. Once an endpoint was reached, pressure in the chamber was increased to -30 mmHg for 1 minute then to 0 for 3 minutes before concluding the study. During the whole LBNP process, the hemodynamic is perturbed, and we demonstrate how the standardization and the proposed algorithm help estimate the phase of the hemodynamic component in the PPG and PVP.

5.2. Results

The PPG and PVP simultaneously recorded from a healthy subject during the LBNP experiment are shown in Figure 2c, where we show the signals during the baseline and during the -75 mmHg pressure (simulating an 1,500cc blood loss). It is clear that for a single subject, the morphologies of the PPG and PVP may be different in different physiological status. In Figure 6a, we show the estimated phases by different bandpass filters with the Hilbert transform, and none of the results is sensible. In Figure 6b, we first show the TFRs of the PPG and PVP by SST. It is

clear that in both TFRs, there is a dominant curve starting at around 1.8Hz, surging to 2.5Hz in the 4/5 of the experiment, and then coming back to 2Hz. This reflects the fact that during a massive blood loss, tachycardia happens. There are more structures in the TFR of the PVP, like a dominant curve at 0.3Hz, and a vague curve around 1Hz from 600sec to 1100sec. The curve at 0.3Hz is associated with the respiration, and the curve around 1Hz from 600sec to 1100sec is unknown and needs more exploration. Moreover, we see that the proposed phase estimation algorithm successfully give a sensible phase and IF, while the IF estimated by differentiating the phase of the PVP signal is noisy. It is not surprising since the PVP signal is usually noisy.

6. Conclusion

Phase is an important quantity to describe an oscillatory signal. In this article, we show that the phase coming from the analytic function model and associated algorithms might not be suitable for biomedical signal analysis. We suggest standardizing the phase definition by modeling oscillatory biomedical time series by the ANHM and applying SST to extract the phase. We demonstrate how to use the proposed algorithm to obtain the standardized phase by applying it to different biomedical time series and provide a Matlab implementation for researchers. If this standardized phase information is properly used, it helps scientific research from different aspects, including information sharing, discussion of the scientific findings among different equipment, and others.

7. Acknowledgments

N/A.

8. References

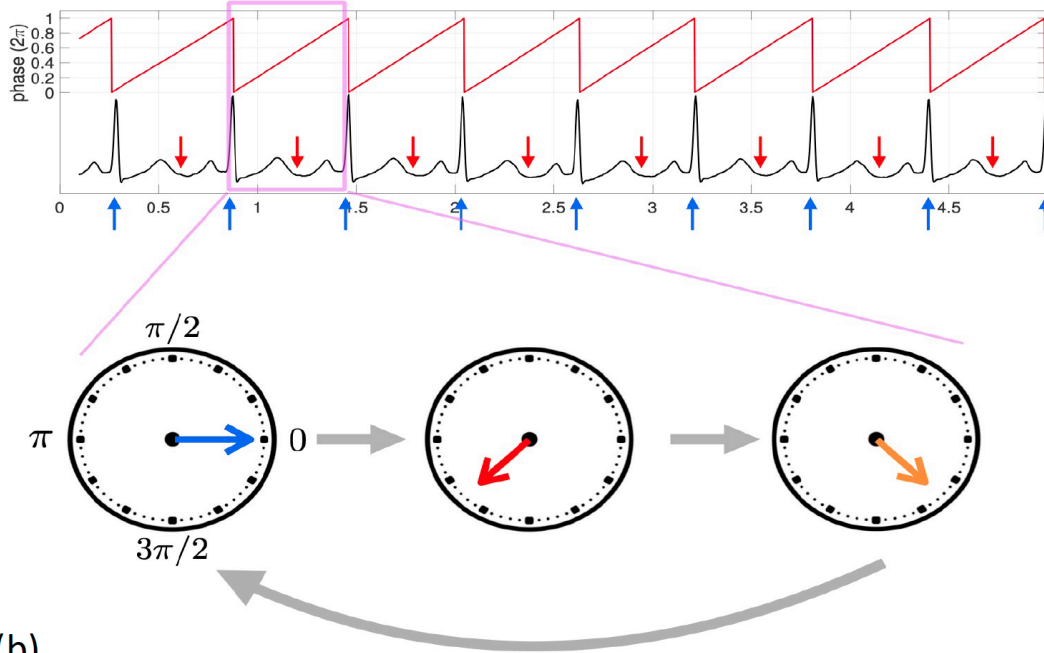
1. Gesche, H., et al., *Continuous blood pressure measurement by using the pulse transit time: comparison to a cuff-based method*. European journal of applied physiology, 2012. **112**(1): p. 309-315.
2. Kim, S.-H., et al., *Beat-to-beat tracking of systolic blood pressure using noninvasive pulse transit time during anesthesia induction in hypertensive patients*. Anesthesia & Analgesia, 2013. **116**(1): p. 94-100.
3. Schäfer, C., et al., *Synchronization in the human cardiorespiratory system*. Physical Review E, 1999. **60**(1): p. 857.
4. Lachaux, J.P., et al., *A quantitative study of gamma-band activity in human intracranial recordings triggered by visual stimuli*. European Journal of Neuroscience, 2000. **12**(7): p. 2608-2622.
5. Khodagholy, D., J.N. Gelineau, and G. Buzsáki, *Learning-enhanced coupling between ripple oscillations in association cortices and hippocampus*. Science, 2017. **358**(6361): p. 369-372.
6. Picinbono, B., *On instantaneous amplitude and phase of signals*. IEEE Transactions on signal processing, 1997. **45**(3): p. 552-560.
7. Van der Pol, B., *The fundamental principles of frequency modulation*. Journal of the Institution of Electrical Engineers-Part III: Radio and Communication Engineering, 1946. **93**(23): p. 153-158.
8. Rihaczek, A. and E. Bedrosian, *Hilbert transforms and the complex representation of real signals*. Proceedings of the IEEE, 1966. **54**(3): p. 434-435.
9. Bedrosian, E., *A product theorem for Hilbert transforms*. 1962.
10. Gabor, D., *Theory of communication. Part 1: The analysis of information*. Journal of the Institution of Electrical Engineers-Part III: Radio and Communication Engineering, 1946. **93**(26): p. 429-441.
11. Nevanlinna, R., *The First Main Theorem in the Theory of Meromorphic Functions*, in *Analytic Functions*. 1970, Springer. p. 162-180.
12. Oppenheim, A.V., *Discrete-time signal processing*. 1999: Pearson Education India.
13. Feldman, M., *Time-varying vibration decomposition and analysis based on the Hilbert transform*. Journal of Sound and Vibration, 2006. **295**(3-5): p. 518-530.
14. Daubechies, I., *Ten lectures on wavelets (SIAM, Philadelphia, 1992)*. MR 93e, 1992. **42045**.
15. Cohen, L., *Time-frequency distributions-a review*. Proceedings of the IEEE, 1989. **77**(7): p. 941-981.
16. Flandrin, P., *Time-frequency/time-scale analysis*. 1998: Academic press.

17. Qian, T., *Intrinsic mono-component decomposition of functions: an advance of Fourier theory*. *Mathematical Methods in the Applied Sciences*, 2010. **33**(7): p. 880-891.
18. Nahon, M.R., *Phase evaluation and segmentation*. 2001.
19. Huang, N.E., et al., *The empirical mode decomposition and the Hilbert spectrum for nonlinear and non-stationary time series analysis*. *Proceedings of the Royal Society of London. Series A: mathematical, physical and engineering sciences*, 1998. **454**(1971): p. 903-995.
20. Chavez, M., et al., *Towards a proper estimation of phase synchronization from time series*. *Journal of Neuroscience methods*, 2006. **154**(1-2): p. 149-160.
21. Le Van Quyen, M., et al., *Comparison of Hilbert transform and wavelet methods for the analysis of neuronal synchrony*. *Journal of neuroscience methods*, 2001. **111**(2): p. 83-98.
22. Chen, Y.-C., M.-Y. Cheng, and H.-T. Wu, *Non-parametric and adaptive modelling of dynamic periodicity and trend with heteroscedastic and dependent errors*. *Journal of the Royal Statistical Society: Series B: Statistical Methodology*, 2014: p. 651-682.
23. Daubechies, I., J. Lu, and H.-T. Wu, *Synchrosqueezed wavelet transforms: An empirical mode decomposition-like tool*. *Applied and computational harmonic analysis*, 2011. **30**(2): p. 243-261.
24. Benchetrit, G., *Breathing pattern in humans: diversity and individuality*. *Respiration physiology*, 2000. **122**(2-3): p. 123-129.
25. Lin, Y.T., et al., *Time-varying spectral analysis revealing differential effects of sevoflurane anaesthesia: non-rhythmic-to-rhythmic ratio*. *Acta Anaesthesiologica Scandinavica*, 2014. **58**(2): p. 157-167.
26. Wu, H.-T., et al., *Respiratory variability during NAVA ventilation in children: authors' reply*. *Frontiers in pediatrics*, 2015. **3**: p. 13.
27. Vakman, D., *On the analytic signal, the Teager-Kaiser energy algorithm, and other methods for defining amplitude and frequency*. *IEEE Transactions on signal processing*, 1996. **44**(4): p. 791-797.
28. Huang, J., Y. Wang, and L. Yang, *Vakman's problem and the extension of Hilbert transform*. *Applied and computational harmonic analysis*, 2013. **34**(2): p. 308-316.
29. Vakman, D., *On the definition of concepts of amplitude, phase and instantaneous frequency of a signal*. *Radio Eng. Electron. Phys*, 1972. **17**(5): p. 754-759.
30. Nuttall, A. and E. Bedrosian, *On the quadrature approximation to the Hilbert transform of modulated signals*. *Proceedings of the IEEE*, 1966. **54**(10): p. 1458-1459.
31. Shelley, K.H., *Photoplethysmography: beyond the calculation of arterial oxygen saturation and heart rate*. *Anesthesia & Analgesia*, 2007. **105**(6): p. S31-S36.
32. Luo, S., W.J. Tompkins, and J.G. Webster. *Cardiogenic artifact cancellation in apnea monitoring*. in *Proceedings of 16th Annual International Conference of the IEEE Engineering in Medicine and Biology Society*. 1994. IEEE.

33. Wu, H.-T., *Instantaneous frequency and wave shape functions (I)*. Applied and Computational Harmonic Analysis, 2013. **35**(2): p. 181-199.
34. Lin, C.-Y., L. Su, and H.-T. Wu, *Wave-shape function analysis*. Journal of Fourier Analysis and Applications, 2018. **24**(2): p. 451-505.
35. Wu, H.-T., *Current state of nonlinear-type time-frequency analysis and applications to high-frequency biomedical signals*. Current Opinion in Systems Biology, 2020. **In press**.
36. Sourisseau, M., H.-T. Wu, and Z. Zhou, *Inference of synchrosqueezing transform--toward a unified statistical analysis of nonlinear-type time-frequency analysis*. arXiv preprint arXiv:1904.09534, 2019.
37. Schäfer, C., et al., *Heartbeat synchronized with ventilation*. nature, 1998. **392**(6673): p. 239-240.
38. Rosenblum, M.G., et al., *Identification of coupling direction: application to cardiorespiratory interaction*. Physical Review E, 2002. **65**(4): p. 041909.
39. Pikovsky, A.S., et al., *Phase synchronization of chaotic oscillators by external driving*. Physica D: Nonlinear Phenomena, 1997. **104**(3-4): p. 219-238.
40. Peltola, M., *Role of editing of RR intervals in the analysis of heart rate variability*. Frontiers in physiology, 2012. **3**: p. 148.
41. Alian, A.A., et al., *Impact of central hypovolemia on photoplethysmographic waveform parameters in healthy volunteers part 2: frequency domain analysis*. Journal of clinical monitoring and computing, 2011. **25**(6): p. 387-396.
42. Wu, H.-T., Alian, A. and Shelley, K., 2020. A new approach to complicated and noisy physiological waveforms analysis: peripheral venous pressure waveform as an example. *Journal of Clinical Monitoring and Computing*, pp.1-17.

Figures

(a)



(b)

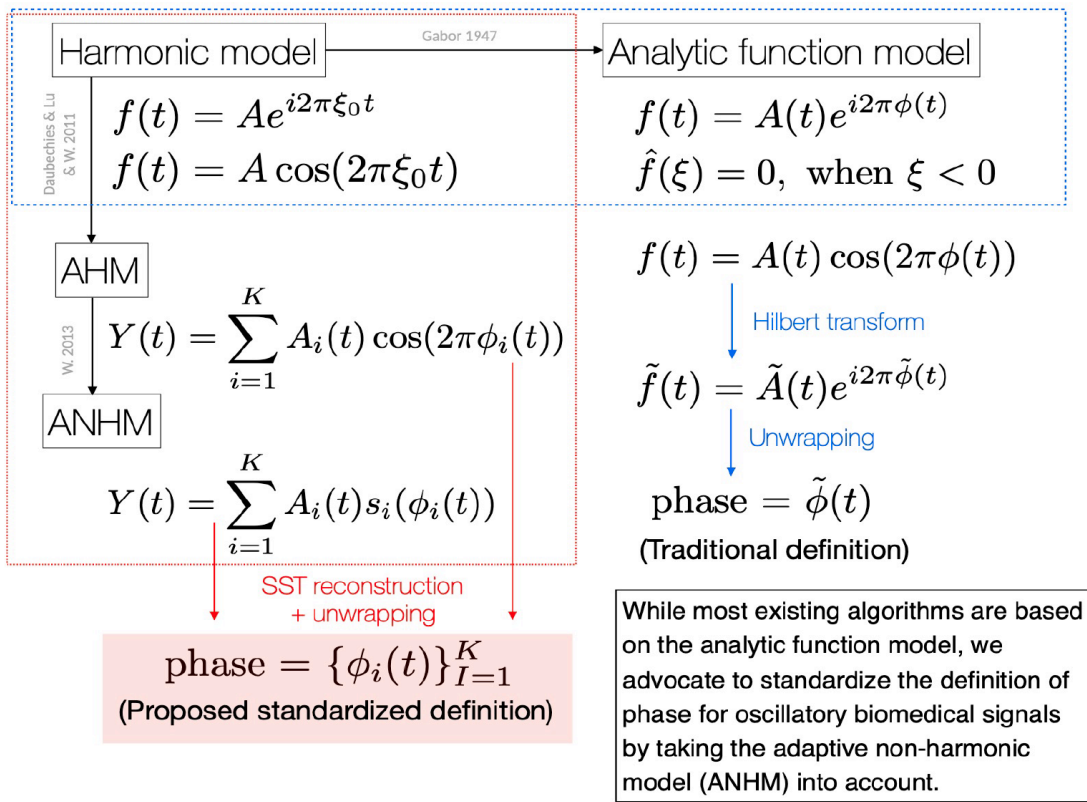


Figure 1: (a) The red curve on the top is the phase function associated with the ECG shown in the black curve, which ranges from 0 to 1 with the unit 2π . The cycle indicated by the magenta box is zoomed in to illustrate the idea of phase with a clock-like circling plot, where the time flow is indicated by the gray arrows. The blue arrows below the ECG signal indicate the status associated the phase 0, and the red arrows above the ECG signal indicate the status associated with the phase $5\pi/4$. The phase 0 is associated with the R peaks, and the phase $5\pi/4$ is associated with the T end. In our proposed standardization, the phase is defined as a monotonically increasing function. This might cause some confusions in the illustrated phase in the red curve. Since the phase is the argument (or the angle) of the complex value, a phase value θ is not different from a phase value $\theta + 2k\pi$ for any integer k . Therefore, one way to plot the phase function is plotting the residue of the phase function by finding its value modulo 2π . (b) A summary of models for the definition of phase function. The traditional phase is shown on the right hand side, and the proposed standardized phase is shown on the left hand side.

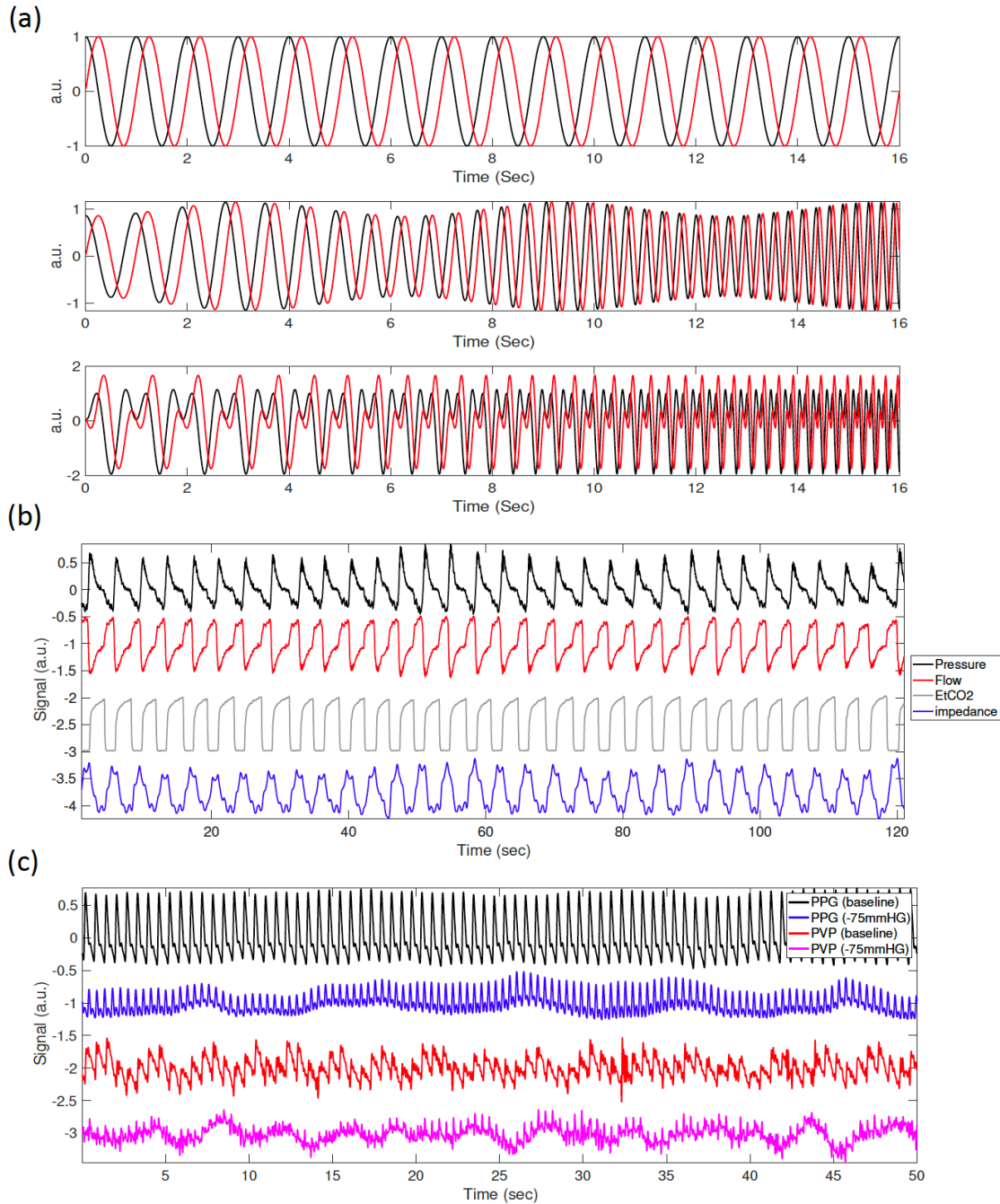


Figure 2: (a) illustration of simulated signals satisfying different models. Top: the harmonic model (1) $f(t) = e^{i2\pi t}$; middle: the adaptive harmonic model (3) $f(t) = (1 + 0.3\cos(t)) e^{i2\pi(t+0.02t^{2.5})}$; bottom: the wave-shape model (5) with $L = 1$, $f(t) = e^{i2\pi(t+0.02t^{2.5})} + 0.95e^{i[4\pi(t+0.02t^{2.5})+3]}$. The black and red curves are the real and imaginary parts of the complex form, respectively. (b) An

illustration of various respiratory signals recorded simultaneously. It is clear that the morphology of those respiratory signals are different, and this difference is mainly encoded in the multiples. (c) An illustration of photoplethmogram (PPG) and peripheral venous pressure (PVP) signals recorded simultaneously during the lower body negative pressure (LBNP) experiment. The four signals from top to bottom are the PPG signal during the baseline, the PPG signal during the -75 mmHg negative pressure, the PVP signal during the baseline, and the PVP signal during the -75 mmHg negative pressure. It is clear that the morphologies of the same channels are different during different physiological status, and this difference is mainly encoded in the multiples.

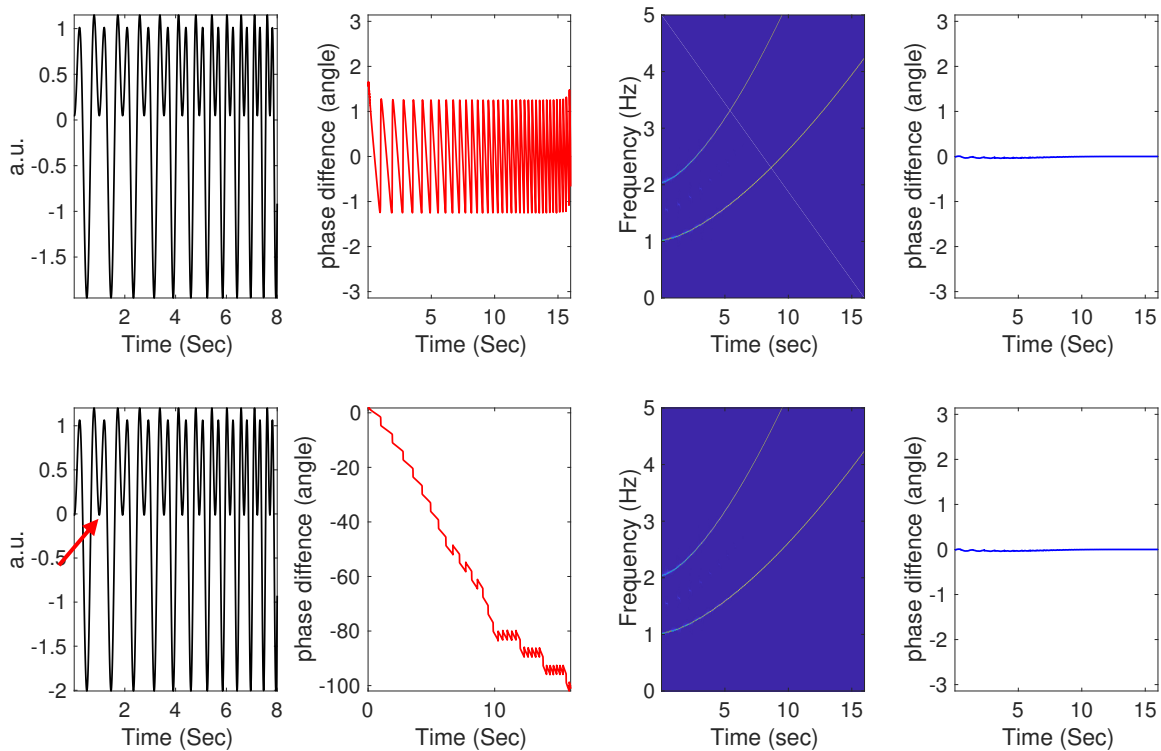


Figure 3: An illustration of the potential problem the Hilbert transform might encounter. The first signal, the real part of $f_1(t) = e^{i2\pi(t+0.02t^{2.5})} + 0.95e^{i[4\pi(t+0.02t^{2.5})+3]}$, is shown on the left top panel, and the second signal, the real part of $f_2(t) = e^{i2\pi(t+0.02t^{2.5})} + 1.01e^{i[4\pi(t+0.02t^{2.5})+3]}$ is shown on the left bottom panel. Note that the real part of $f_2(t)$ crosses zero due to the fact that the first harmonic has a larger amplitude than the fundamental component (red arrows). In the left middle

columns, the red lines are the difference of the phase of the fundamental component, $\varphi(t) = 2\pi(t + 0.02t^{2.5})$, and the estimated phase $\tilde{\varphi}(t)$ by directly applying the Hilbert transform. It is clear that for $f_1(t)$, there is an obvious zig-zag difference between the estimated phase function $\tilde{\varphi}(t)$ and the proposed phase function $\varphi(t)$. However, for $f_2(t)$, there is an obvious cumulative phase estimation error as time evolves. This comes from the winding number issue due to the larger amplitude of the first harmonic. Due to the frequency modulation, the bandpass filter or continuous wavelet transform does not work as well (results not shown). In the right middle columns, the time-frequency representations of $f_1(t)$ and $f_2(t)$ determined by the synchrosqueezing transform (SST) are shown. In the right column, the blue lines are the difference of the estimated phase by SST and the proposed phase function $\varphi(t)$. It is clear that despite the winding issue, SST provides a consistent phase estimation.

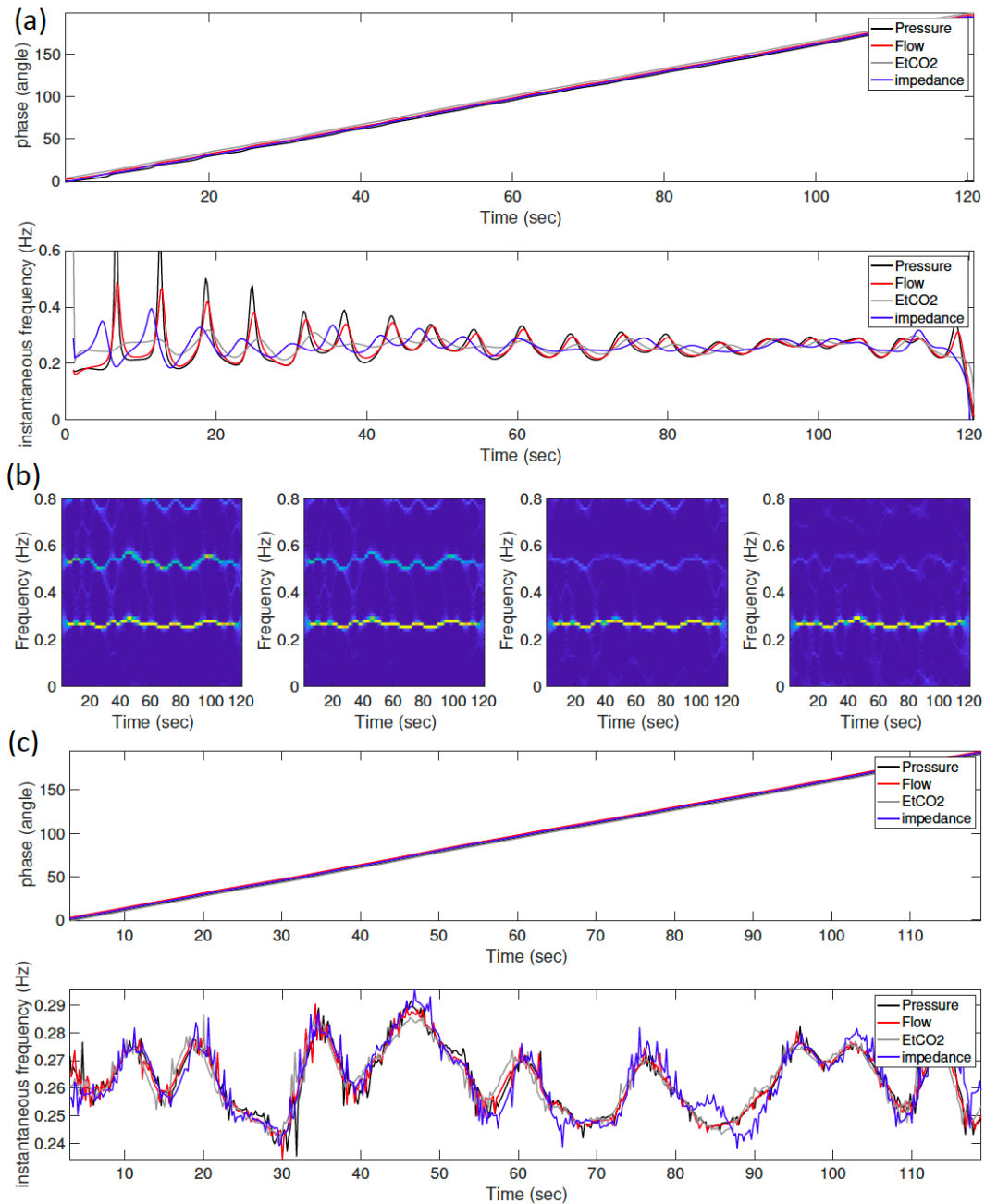
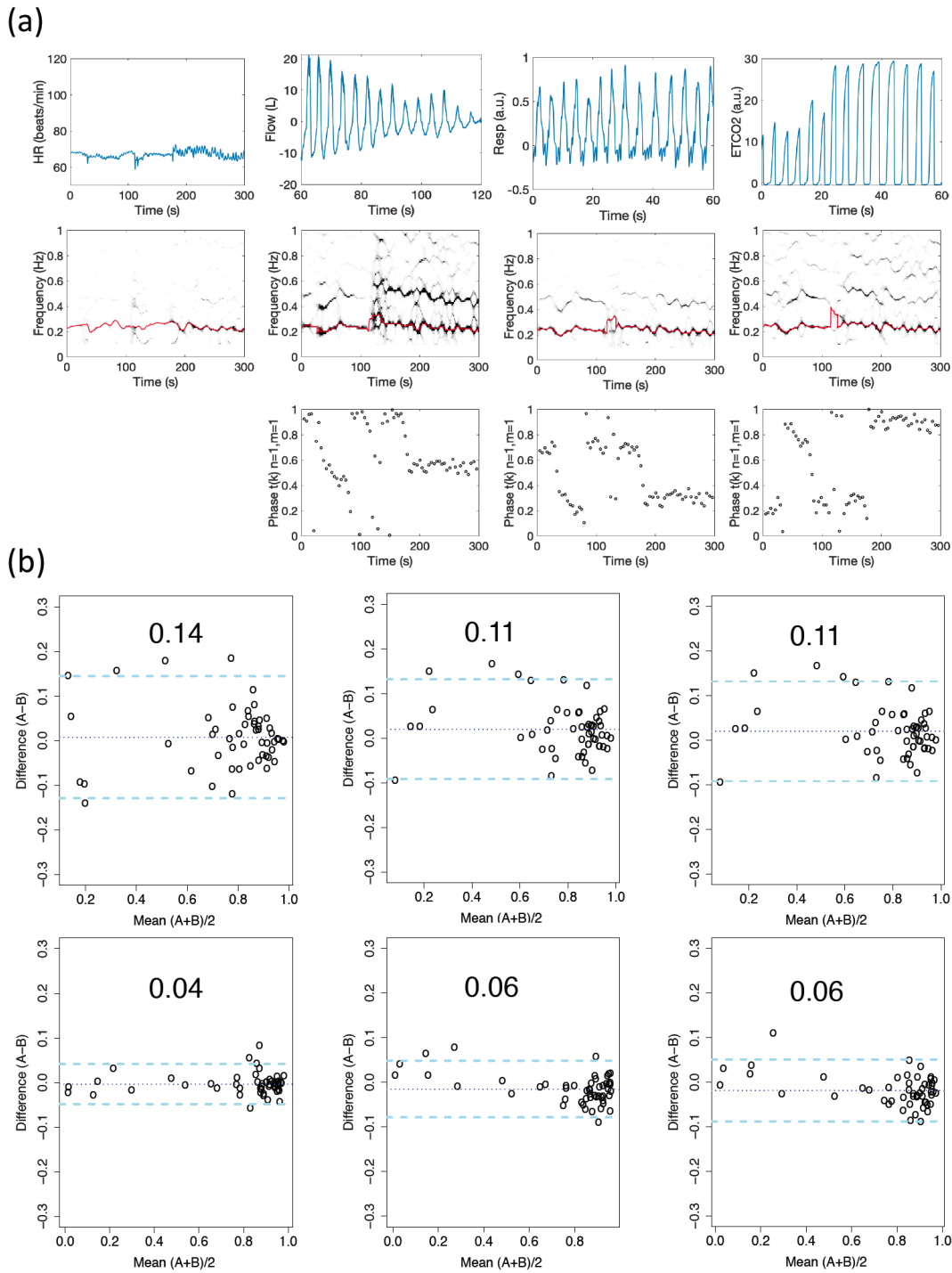
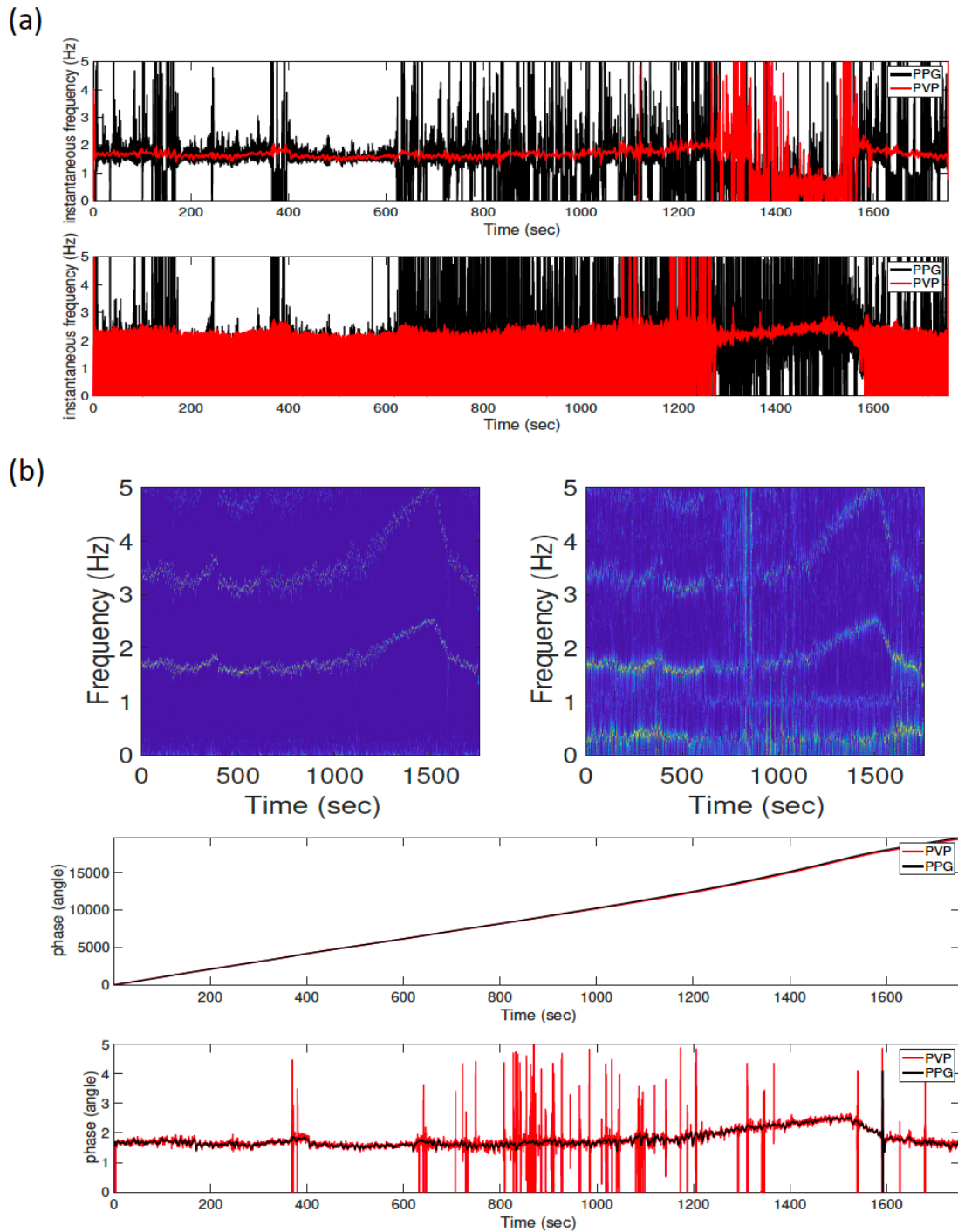


Figure 4: (a) An example of determining phases of various respiratory signals by the Hilbert transform of the band-pass filtered respiratory signals. The band is 0.1-0.4 Hz determined by the dominant respiratory frequency. It is clear that the phases, and hence their derivatives, are not consistent from one channel to another one. More importantly, while the definition of instantaneous frequency is mathematically correct, physiologically it is not sensible. (b) An example of determining phases of various respiratory signals by the Synchrosqueezing transform

(SST). From left to right: the time-frequency representations of the pressure, flow, end-tidal CO₂, and impedance signals determined by SST. (c) Top panel: the phases of four respiratory signals. Bottom panel: the instantaneous frequency of four respiratory signals. It is clear that the phases of different respiratory signals are consistent, except a global phase shift. Also, the derivatives, which is the instantaneous frequency by our definition, are consistent.



by the synchrogram. Top row, from left to right: the instantaneous heart rate (IHR), the flow signal, the impedance signal, and the end-tidal CO₂ (EtCO₂) signal. Middle row, from left to right: the time-frequency representation of the associated signal shown in the top row determined by the synchrosqueezing transform. Bottom row, from left to right: the synchrograms of the IHR and flow, the IHR and impedance, and the IHR and EtCO₂, respectively. (b) Bland-Altman plot of the cardiopulmonary coupling index determined from different phase reconstruction methods and different respiratory signals. From left to right: the comparison of impedance and end-tidal CO₂ (EtCO₂), the comparison of impedance and flow, and the comparison of EtCO₂ and flow. Top row: the phases are determined by the Hilbert transform. Bottom row: the phases are determined by SST. The standard deviation of each comparison is shown in the plot.



signals. On the top panel, the band is 0.5-2 Hz determined by the dominant cardiac oscillatory frequency; it is clear that the phases, and hence their derivatives, are not consistent between the PPG and PVP signals. More importantly, while the definition of instantaneous frequency is mathematically correct, physiologically it is not sensible. This comes from the fact that the heart rate changes from one status to another during the lower body negative pressure experiment.

(b) An example of determining phases of hemodynamics from various physiological signals by the Synchrosqueezing transform (SST). Top panel, from left to right: the time-frequency representations of the photoplethmogram (PPG) and peripheral venous pressure (PVP) signals determined by SST. Middle panel: the phases of PPG and PVP signals. Bottom panel: the instantaneous frequency of the hemodynamic oscillation determined by differentiating the estimated phases associated with the PPG and PVP signals. It is clear that the phases of PPG and PVP signals are consistent. Also, the derivatives, which is the instantaneous frequency by our definition, are consistent, except some unwanted spikes in the PVP signal. This comes from the well-known fact that the PVP signal is usually too noisy to analyze with traditional tools.